BioResearch Open Access
Volume 3, Number 3, June 2014

DOI: 10.1089/biores.2014.0015

Surface Entrapment of Fibronectin on Electrospun PLGA Scaffolds for Periodontal Tissue Engineering

Doris M. Campos,[1,2] Kerstin Gritsch,[1–3] Vincent Salles,[1] Ghania N. Attik,[1] and Brigitte Grosgogeat[1,2,4]

Abstract

Nowadays, the challenge in the tissue engineering field consists in the development of biomaterials designed to regenerate *ad integrum* damaged tissues. Despite the current use of bioresorbable polyesters such as poly(L-lactide) (PLA), poly(D,L-lactide-*co*-glycolide) (PLGA), and poly-ε-caprolactone in soft tissue regeneration researches, their hydrophobic properties negatively influence the cell adhesion. Here, to overcome it, we have developed a fibronectin (FN)-functionalized electrospun PLGA scaffold for periodontal ligament regeneration. Functionalization of electrospun PLGA scaffolds was performed by alkaline hydrolysis (0.1 or 0.01 M NaOH). Then, hydrolyzed scaffolds were coated by simple deposition of an FN layer (10 μg/mL). FN coating was evidenced by X-ray photoelectron analysis. A decrease of contact angle and greater cell adhesion to hydrolyzed, FN-coated PLGA scaffolds were noticed. Suitable degradation behavior without pH variations was observed for all samples up to 28 days. All treated materials presented strong shrinkage, fiber orientation loss, and collapsed fibers. However, functionalization process using 0.01 M NaOH concentration resulted in unchanged scaffold porosity, preserved chemical composition, and similar mechanical properties compared with untreated scaffolds. The proposed simplified method to functionalize electrospun PLGA fibers is an efficient route to make polyester scaffolds more biocompatible and shows potential for tissue engineering.

Key words: biomaterials; proteins; tissue engineering

Introduction

The progressive advances and challenges in tissue engineering (TE) succeed the creation of adapted scaffold designs to promote the successful tissue regeneration *in vivo*.[1–3] Despite all current researches performed in periodontics to *ad integrum* regenerate the periodontal tissues, to date there are no clinical solutions to repair periodontium once periodontitis becomes established.[4–6] Composed of four dental tissues (i.e., gingiva, alveolar bone, cementum, and periodontal ligament [PDL]), the periodontium is constantly maintained by the progenitor PDL cells through their great capacity of differentiation into cementoblasts, odontoblasts, and fibroblasts.[7–10] PDL plays a key role in the attachment of teeth to the jaw; in the most drastic cases of periodontitis—in which a chronic inflammation sets in—PDL destruction could lead to the loss of the tooth.[4,11] With the wish to expand TE therapeutics for a higher number of patients, acellular biomaterials may be employed as a novel approach to heal periodontal site by the active recruitment of patient cells into the PDL scaffold in order to provide *in situ* regeneration in the cases of periodontitis.[3,12]

In periodontal TE application, scaffolds degradability is an important parameter during wound healing process. Biodegradable polyesters such as poly(L-lactide) (PLA), poly(D,L-lactide-*co*-glycolide) (PLGA), and poly-ε-caprolactone have shown promising results in *in vivo* studies.[1–3] Because of their suitable degradability rate, PLGA scaffolds have been studied as conductive/inductive graft material without cytotoxicity or toxic waste degradation products.[13–15] Showing similar fibrous structure to natural extracellular matrix (ECM), designed PLGA electrospun random and oriented fibrous frameworks have been proposed as mechanical support to guide cell migration through the material in different TE applications.[16–19] However, to obtain great biocompatibility properties, PLGA scaffolds should be functionalized to decrease their hydrophobicity and to mediate cells in the first recognition and attachment.[20,21]

Several authors have performed a successful immobilization of adhesive molecules such as laminin, collagen, and gelatin onto polyester-based biomaterials in order to reduce their hydrophobicity and to increase their biocompatibility.[20–23] In this sense, the use of ECM proteins such as fibronectin (FN) may enhance cell recognition and the ability of the surface to

[1]Laboratoire des Multimatériaux et Interfaces CNRS UMR 5615; [2]UFR d'odontologie; [3]Centre de Soins, d'Enseignement et de Recherche Dentaires (Département de Parodontologie); and [4]Centre de Soins, d'Enseignement et de Recherche Dentaires (Département de Santé Publique), Université Lyon 1, Villeurbanne, France.

become colonized by the surrounding cells via its RGD (Arg-Gly-Asp) domains. FN is a ligant–integrin affinity protein found in the mammalian ECM. The chemical surface modification obtained by FN deposition is able to create sites for cell recognition by specific integrin bindings facilitating cell–material interactions.[23–26] Although many surface modification methods have been proposed, the deposition of biomacromolecules on the PLGA surface requires intermediary molecules, organic coupling agents, and multiple steps to ensure the bioactive surface functionalization.[20,22] Moreover, a complex functionalization with multiple steps might result in difficulty in producing sterile medical devices.

Herein, a simplified surface functionalization by FN deposition onto hydrolyzed PLGA fibers is proposed as a novel way to make scaffolds more bioactive. To fabricate a biomaterial as close as possible to PDL matrix, PLGA frameworks are manufactured using a rotary co-electrospinning method. Two concentrations of sodium hydroxide were tested in order to active electrospun fibers. The physical, chemical, and structural modifications after treatment were studied and compared with untreated scaffolds. The functionalized scaffolds' biocompatibility and capacity to become colonized were also investigated.

Materials and Methods

Fabrication of electrospun PLGA scaffolds

PLGA with a molar ratio of 50:50 (Mn 30,000–60,000; inherent viscosity 0.55–0.75 dL/g; Sigma-Aldrich) fibers were fabricated using a rotary cospinning method to get a mat of oriented filaments giving mechanical properties.[27] PLGA polymer was dissolved in anhydrous dichloromethane solvent (DCM; molecular weight 84.93 g/mol, density 1.325 g/cm^3; Sigma-Aldrich) at a concentration of 20% (w/v) to obtain a homogeneous solution. Two 21-gauge needles were placed in opposite directions at 10 cm tip-to-target distance, and the polymer solutions were extruded simultaneously at a feeding rate of 6 mL/h. PLGA filaments were collected as a deposited membrane onto an aluminum foil (10×10 cm^2) fixed on a rotating cylindrical target ($Ø = 11$ mm; at 1060 rad/min). Required potential difference was generated by a high-voltage supplier using ± 12 kV of electrical potential at each needle (opposite potential). The target rotation was maintained for 5 h after spinning to obtain homogeneous DCM evaporation in order to limit crack formation in the mat. The environmental conditions were fixed at 20°C and 30% of humidity.

PLGA hydrolysis and protein functionalization

Sodium hydroxide (NaOH; Merck) was used to hydrolyze PLGA scaffolds. Samples were cut (1 cm^2) and hydrolyzed by NaOH solutions at 0.01 and 0.1 M (1 M is not included in this study since it dissolves the sample in a few minutes) in distilled water for 20 min at 37°C. A time of 20 min was chosen because the results obtained for the immersion times 20, 40, and 60 min were similar as described before by Croll et al.[28] Then, they were rinsed twice with phosphate buffered saline (PBS; pH 7.4) for 5 min each. After the hydrolysis reaction, an FN solution (at 10 μg/mL in PBS) from human plasma (Sigma-Aldrich) protein coating was deposited on untreated and hydrolyzed PLGA fibers for 24 h at 37°C. Longer deposition times (48 and 72 h) were also investigated, leading to equivalent results in terms of coating quality but to higher shrinkage. Samples without FN deposition were immersed in PBS to simulate the same conditions. After 24 h, all group samples were rinsed twice with PBS and dried for 3 days in a desiccator. Sample groups are described in Table 1.

Scaffold morphology and physical characterization

PLGA scaffold groups were observed by scanning electron microscopy (SEM; Quanta 250^{TM}; FEI Co.). Dried samples were coated with a $\sim$8 nm gold–palladium film by sputtering at room temperature. Pictures were taken under high vacuum at 80×, 500×, 1000×, and 2500× magnifications with 5 kV. Using SEM digital micrographs and ImageJ 1.45s software, scaffold morphology, alignment, and fiber diameter were characterized. For surface porosity measurements, binary images were created using ImageJ 1.45s software, and the area of the black parts (pores) was estimated by measuring the shortest and the longest diagonals of each ellipse corresponding to the shape of the pore. The pore size was finally an average of 10 measurements. The preferential orientation of PLGA fibers was calculated using fast Fourier transform in SEM images as described by Ayres et al.[29] The shrinkage of scaffold samples was determined by the area modification measurements. Six samples from each sample group were previously measured and compared with their untreated PLGA initial area: Shrinkage (%) $= (1 - A/A_0) \times 100$, where A is dried PLGA area after treatment and A_0 is untreated PLGA initial area. Hydrophobicity analysis was obtained by contact angle measurements of untreated and treated PLGA scaffolds in air on the surface of the samples using DSA3 software (Kruss; Easy Drop). Different sites ($n = 10$) from each group were performed using deionized water—one drop (3 μL) per site. An untreated sample immersed for 24 h in PBS served as control of the effect of temperature and hydration. The temperature and humidity levels were 22°C and 42%, respectively.

Scaffold chemical characterization

All PLGA scaffolds were chemically characterized by attenuated total reflectance Fourier transform infrared (ATR-FT-IR; Spectrum One apparatus; ABB Bomem Inc.) and X-ray photoelectron (XPS; PHI Quantera SXM; Chanhassen) spectroscopies. FT-IR spectra were collected from 4000 to 400 cm^{-1}, using a nominal resolution of 4 cm^{-1} and a number of scans that is equal to 100. XPS spectra were recorded on 3 nm of analyzed surface layer. All chemical elements, except

Table 1. Electrospun PLGA Scaffold Groups

Sample groups	*Chemical treatment*	*Fibronectin deposition*
PLGAH01	NaOH (0.1 M)	PBS
PLGAH001	NaOH (0.01 M)	PBS
PLGAH01FN	NaOH (0.1 M)	FN (10 μg/mL)
PLGAH001FN	NaOH (0.01 M)	FN (10 μg/mL)
PLGA + FN	PBS	FN (10 μg/mL)
PLGA + PBS	PBS	PBS

FN, fibronectin; PBS, phosphate buffered saline; PLGA, poly(D,L-lactide-*co*-glycolide).

H and He, could be visualized with 0.1–0.5% for the atomic detection and 2–5% of precision in concentric hemispherical regions. The content of C, O, N, P, Na, and Cl elements and the O/C were determined on a surface area of 200 μm diameter. Untreated PLGA samples were immersed in PBS for 24 h, and FN-deposited PLGA samples without hydrolysis were included as control samples for comparison (Table 1).

Scaffold mechanical behavior

The mechanical properties of the untreated and treated groups were evaluated by uniaxial tensile testing (MTS Synergy 400®). Scaffolds were cut into rectangles (25 mm × 10 mm) and tested following the direction along the length of the filaments at a cross-head speed of 1 mm/min. Four specimens from each sample group were tested. Tensile modulus (E), ultimate strength (σ), and break elongation (ε) were calculated based on the tangent of the stress–strain curve.

Scaffold degradation

In vitro degradation assay was carried out by incubating samples in an aqueous environment (adapted experimental method based on Zhang et al.[26]). Three specimens of 1 cm^2 ($\sim$4 mg) were separately immersed in 4 mL of PBS for 28 days at 37°C in static condition. Weekly (at 7, 14, 21, and 28 days), the water absorption, mass remain, pH value variations, and scaffold morphology were controlled. For water adsorption and remaining mass measurements, Equations 1 and 2 were employed, respectively:

$$\text{Water absorption } (\%) = (m_{t,w} - m_t)/m_t \times 100 \quad (1)$$

$$\text{Mass remain } (\%) = m_t/m_0 \times 100 \quad (2)$$

where $m_{t,w}$ is the wet mass, m_t is the dried mass (after 7 days in the desiccator), and m_0 is the original mass of the scaffold. Scaffold morphology was observed by SEM. For pH value variations, pH values from incubated PBS were weekly measured using a standard pHmeter (PHM2010; Multilab Radiometer Analytical).

Scaffold biocompatibility

Human PDL (hPDL) fibroblasts were provided by the Laboratory of Biomaterials at the School of Dental Medicine of University of Geneva. When the hPDL cells reached confluence, they were detached with trypsin-EDTA (PAA GE Healthcare), counted, and resuspended in the culture medium of DMEM with stable L-glutamine (PAA GE Healthcare) containing 10% fetal bovine serum (PAA GE Healthcare), 100 U/mL penicillin G, 100 μg/mL streptomycin sulfate (PAA GE Healthcare), and 2 mL/L amphotericin B (PAA GE Healthcare). The medium was renewed 3 × a week. The biocompatibility of the treated scaffolds giving the best results was evaluated and compared with that of nontreated PLGA materials. Samples of 1 cm^2 were sterilized by ultraviolet radiation for 20 min. hPDL fibroblasts in 2nd passage were seeded onto the scaffolds at a density of 10,000 cells/cm^2 by adding 500 μL of cell suspension media and were incubated for 1, 3, or 7 days under standard conditions at 37°C and 5% CO_2.

Quantitative analyses were averaged for 24 h. Cell mitochondrial activity was measured using the amount of Resazurin (Sigma-Aldrich) intensity excitation at 530 nm and emission at 580 nm (Infinite® F200; Tecan Group Ltd.) (n = 3). As a negative control, Resazurin was added to the PBS without cells. For SEM observations, seeded samples were fixed with glutaraldehyde (4%) and paraformaldehyde (2%) in 0.1 M sodium cacodilate buffer (pH 7.4) during 1 h at room temperature. They were then dehydrated and dried by immersion in ethanol and hexamethyldissilazane (HMDS) (Sigma-Aldrich) solutions. The samples were coated with an $\sim$8 nm gold–palladium film and observed by SEM.

The ability of functionalized scaffolds to be colonized by hPDL cells was observed using a confocal laser scanning microscope (FV10i; Olympus). After 24 h of culture, seeded samples were fixed for 1 h in 4% formaldehyde in PBS followed by further washing. The cells were permeabilized with 1% Triton X-100 (Sigma-Aldrich) in PBS and then blocked with 1% PBS/BSA (Sigma-Aldrich). Actin microfilaments were stained by Alexa Fluor 488 phalloidin (at 1:100; Invitrogen) and cell nuclei were identified by propidium iodide (at 1:3000; Invitrogen) at room temperature. Regular images of 1024 × 1024 pixels (0.231 μm × 0.231 μm pixel size) were obtained with a 60 × lens. The images were stored as 12-bits/pixel TIFF files and analyzed with FV10-ASW 3.1 software (Olympus).

Statistical analysis

All quantitative data are presented as mean ± standard deviation (SD). After the Shapiro–Wilk normality test, one-way ANOVA and Tukey *post hoc* tests were performed to determine the statistical significance between the experimental groups. A value of $p < 0.05$ was considered to be statistically significant.

Results

Scaffold functionalization and physical characterization

To propose an optimal framework to PDL regeneration, we performed a co-electrospinning of PLGA solution. PLGA electrospun scaffolds (317 ± 5 μm of thickness) presented highly preferential oriented fibers (Fig. 1A). Structural modification was observed after scaffold hydration in PBS for 24 h at 37°C (Fig. 1B). The morphology of the hydrolyzed fibers differed from the untreated. When treated with higher NaOH concentration (PLGAH01), the fibers became collapsed and broken (Fig. 1C). Samples treated with lower NaOH concentration (PLGAH001) exhibited similar morphology of hydrated nonhydrolyzed scaffolds with relative fiber orientation loss (Fig. 1D). After FN coating, fibers mainly maintained their initial morphology (Fig. 1E,F). It was possible to visualize some thin structures between the PLGA fibers in the PLGAH001FN group (Fig. 1F, black arrows).

Structural modifications led to loss of preferential fiber orientation (Fig. 2). Irregular alignment was evident after scaffold hydration, hydrolysis, and FN functionalization (Fig. 2B–F). For the PLGAH01 and PLGAH01FN, porosity results (Fig. 2H) indicated that the space between the fibers became significantly larger, thus generating overlapping sheets on heterogeneous regions of surface (Fig. 2C). Despite of collapsed morphology, no significant difference in fiber diameter was found between PLGAH01 groups and untreated fibers (Fig. 2G). PLGA H001FN showed fibers with a significantly larger diameter compared with both of PLGAH01 groups (Fig. 2G).

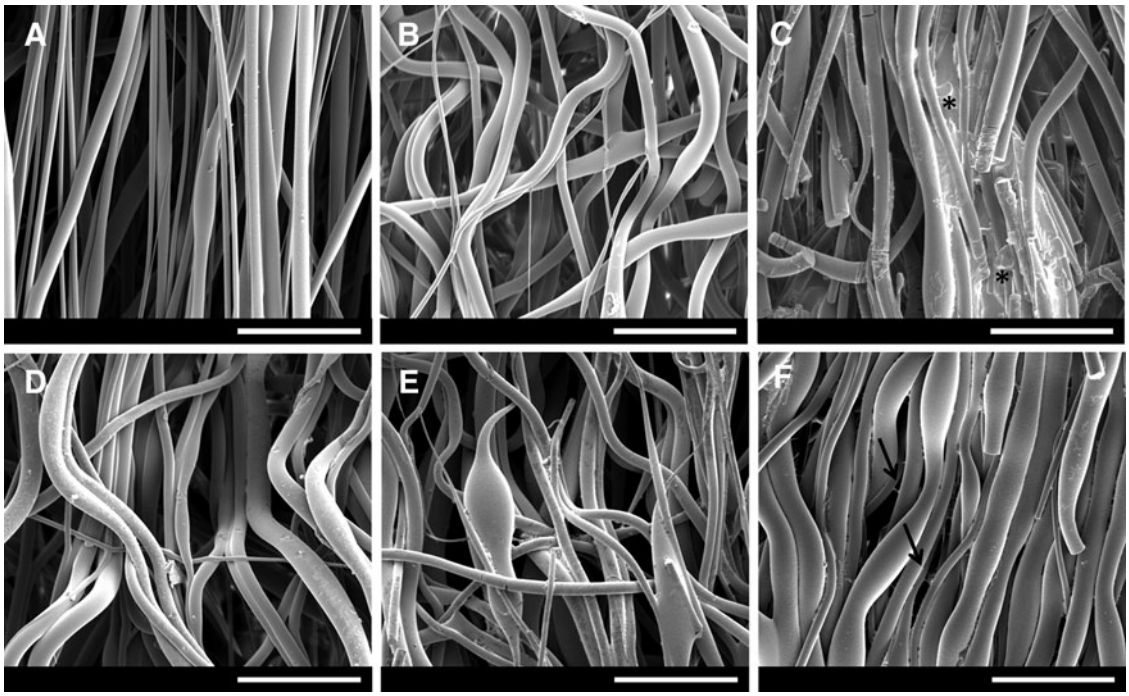

FIG. 1. SEM micrographs of electrospun PLGA scaffolds and treated groups: **(A)** PLGA, **(B)** PLGA PBS, **(C)** PLGAH01, **(D)** PLGAH001, **(E)** PLGAH01FN, and **(F)** PLGAH001FN. Scale bar, 50 μm. Asterisk (*) corresponds to hydrolyzed collapsed fibers; black arrows correspond to deposited structures between PLGA fibers. FN, fibronectin; PBS, phosphate buffered saline; PLGA, poly(D,L-lactide-*co*-glycolide); SEM, scanning electron microscopy.

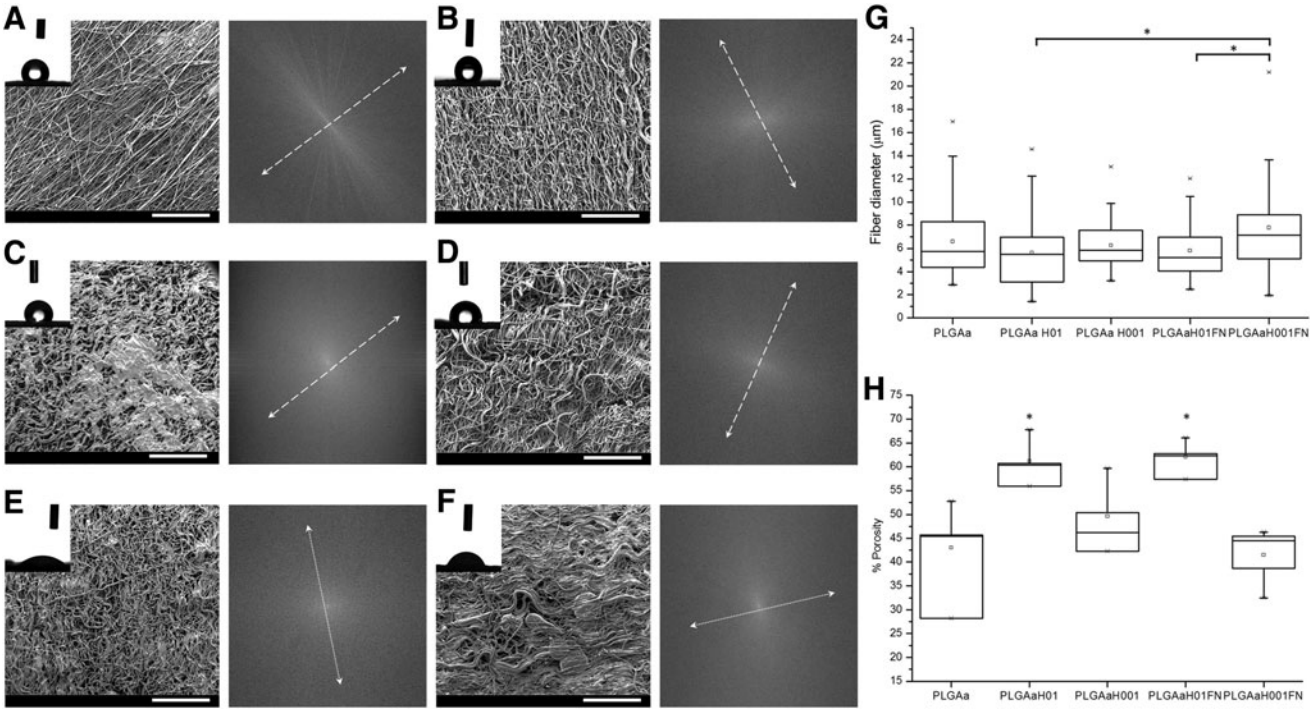

FIG. 2. **(A–F)** SEM micrographs, contact angle water drop images, and fiber orientation (arrows) of electrospun PLGA groups: **(A)** PLGA, **(B)** PLGA PBS, **(C)** PLGAH01, **(D)** PLGAH001, **(E)** PLGAH01FN, and **(F)** PLGAH001FN. SEM scale bar, 500 μm. **(G)** Fiber diameter and **(H)** scaffold porosity of untreated and treated PLGA fibers measured by image treatment. Data are expressed as mean ± SD. *Significant difference between groups ($p < 0.05$).

Table 2. Shrinkage, Initial Mass, Mass After Treatment, and Water Absorption of Electrospun PLGA Scaffolds

Sample groups	*Shrinkage (%)*	*Initial mass (mg)*	*Mass after treatment (mg)*	*Water absorption (%)*
PLGA	0	4.11 ± 0.77	0	0
PLGAH01	14	4.52 ± 0.65	21.24 ± 2.5	373.7 ± 55.5
PLGAH001	19	4.34 ± 0.54	5.4 ± 0.86	24.3 ± 11.6
PLGAH01FN	27	4.3 ± 0.71	21.28 ± 4.6	402.8 ± 108.5
PLGAH001FN	36	4.2 ± 0.55	6.7 ± 1.3	61.1 ± 32.9

Data are expressed as mean ± SD.

The untreated PLGA scaffolds showed higher hydrophobicity with a contact angle of 129.7 ± 6°, followed by hydrated PLGA with 130.1 ± 2° (Fig. 2 A,B). After alkaline hydrolysis reaction, the contact angles are not significantly affected for samples without FN coating (PLGAH01 and PLGAH001). However, the effect of FN clearly shows a decrease of contact angle and an improvement of the surface energy to 22.9 ± 31° for PLGAH01FN and to 64.9 ± 11.8° for PLGAH001FN (Fig. 2E and F, respectively).

From Table 2, dimensional measurements evidenced an important shrinkage in all samples in contact with aqueous solution. Submitted to a humid environment, hydrolyzed samples suffered 14% and 19% of shrinkage (for PLGAH01 and PLGAH001, respectively) compared with untreated PLGA. A higher shrinkage behavior of 27% and 36% was measured at FN-coated surfaces of PLGAH01FN and PLGAH001FN groups, respectively. The reactions in an aqueous environment and the consequent water molecules adsorption have resulted in a significant increase of the remaining mass for PLGAH01 samples, with a water adsorption percentage of approximately 373% for PLGAH01 and 402% for PLGAH01FN. This behavior was not observed for PLGAH001 and PLGAH001FN groups.

Polymer stability and protein coating

Hydrolysis may induce chemical modifications, and the preservation of PLGA chains was verified by ATR-FT-IR and XPS. Typical spectra of PLGA polymer-based material were found from ATR-FT-IR and XPS analysis for all analyzed groups (Fig. 3 A,B). By FT-IR, a strong ether carbonyl stretch (C = O) absorption band of the PLGA group was found at 1747 cm^{-1}; ether group stretching (C–O–C) at 1083 cm^{-1} and methyl stretching (C–H) and (C–CH_3) groups at 1450 and 1043 cm^{-1}, respectively, were also found. These bands could also be observed in the all FT-IR spectra from the hydrolyzed, coated scaffolds without other significant changes. From XPS results, all spectra were similar between groups with C–C and C–H of C1s at 285 eV. The N1s pic corresponding to N–C organic bindings was detected at 399.7 eV. From both of the hydrolyzed, FN-coated samples' spectra, a pic at 401.7 eV was visualized and corresponds to N = O bindings. The presence of the P2p pic in phosphate form was detected at 133.5 eV, and it may be related to PBS. Similarly, the spectrum of PLGA PBS presented pics of Na and Cl elements, probably from the PBS. The elementary composition of PLGA chains was also evidenced by the similar O/C values (Table 3). Even if a lower O/C value visualized for PLGAH001FN groups was because of the lower presence of oxygen at the sample surface, higher values of carbon and nitrogen percentage were observed: 61.1% and 3.3%, respectively (Table 3).

Mechanical properties and degradability behavior

The results of the mechanical properties are summarized in Figure 4. Compared with untreated PLGA scaffolds, hydrolysis treatment caused a significant decrease in the tensile

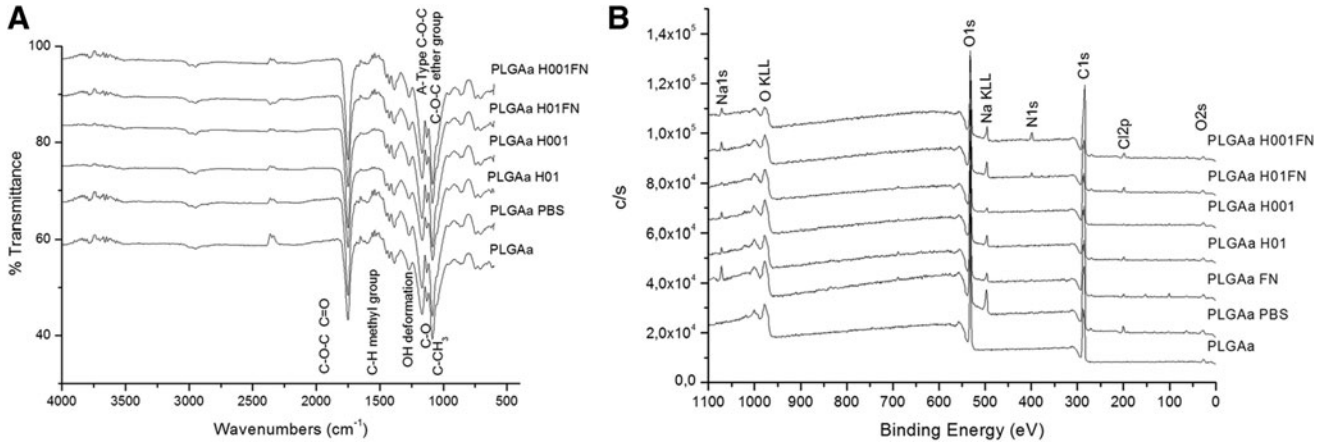

FIG. 3. Chemical characterization of untreated, hydrolyzed, and hydrolyzed-and-coated PLGA scaffolds by **(A)** ATR-FT-IR and **(B)** XPS spectra. Control groups: PLGA scaffold immersed in PBS (PLGA PBS) and in fibronectin solution (PLGA FN) for 24 h. ATR-FT-IR, attenuated total reflectance Fourier transform infrared; XPS, X-ray photoelectron spectroscopy.

Table 3. Chemical Elements Percentage and O/C Values of Electrospun PLGA Scaffolds

	C	*O*	*N*	*P*	*Na*	*Cl*	*O/C*
PLGA	56.6	43.3	0	0	0	0	0.77
PLGA PBS	55.9	38.9	0.2	0.4	2.3	1.1	0.70
PLGA FN	54.7	40.2	0.5	0.1	0.8	0.6	0.71
PLGAH01	56.3	41.0	0.1	0.2	0.9	0.6	0.73
PLGAH001	58.3	40.6	0	0	0.2	0.2	0.70
PLGAH01FN	57.03	38.5	1.6	0.3	1.4	1.0	0.67
PLGAH001FN	61.1	32.6	3.3	0.2	1.3	1.0	0.53

modulus from 75 ± 14 MPa for PLGA group to 45 ± 22 MPa for PLGAH01 and to 65 ± 19 MPa for PLGAH001. The presence of FN coating was significant to decrease mechanical properties: to 13.2 ± 7.8 MPa for PLGAH01FN and to 15.9 ± 3.4 MPa for PLGAH001FN (Fig. 4).

Loss of fiber alignment, fiber scissions, and loss of porosity during the hydrolysis degradation process were observed during *in vitro* degradation assay up to 28 days (Fig. 5). PLGA scaffold groups suffered a loss of mass and strong structural modifications. The mass of untreated PLGA scaffolds was stable up to 28 days (Fig. 5I). In general, the profiles from treated PLGA scaffolds presented an increase in scaffold mass during the first week, followed by a decrease in mass behavior (Fig. 5I). No important mass variations in measurements were observed for PLGAH001 and PLGAH001FN samples. A weekly morphological evolution of untreated PLGA scaffolds is shown in Figure 5A–E. More hydrophilic PLGAH001FN samples have shown typically and more significant shrinkage behavior with loss of porosity during scaffold degradation (Fig. 5F–H). In detail, these hydrolyzed, coated fibers became collapsed (Fig. 5J-i, black arrows), with the presence of heterogeneous pores (from 497.1 nm to 3.279 μm in diameter) on the PLGA fiber surface up to 21 days (Fig. 5 J-ii, iii). The presence of pores was intensified during degradation assay progression (data not shown). From the pH value variation, the results showed no drastic changes in the pH values for any of the groups (Fig. 5K).

Scaffold biocompatibility observations

Physical and chemical characterizations were performed to propose an optimal functionalized scaffold to PDL TE application. From these results, the PLGAH001FN group was selected to verify the capacity of alkaline hydrolysis and FN coating to improve biocompatibility properties. From SEM micrographs (Fig. 6 A,B), PDL cells were able to adhere on both sample surfaces: untreated PLGA and PLGAH001FN samples. However, PDL cells showed round-shape and unspread morphology at the untreated PLGA surface (Fig. 6A). In contrast, when cells were cultured on PLGAH001FN surface, cell adhesion structures were visualized with spread morphology and all surface was homogenously colonized by cells (data not shown). Some observed structures may be related to a novel ECM deposition (Fig. 6B). To demonstrate the capacity of cells to migrate through the scaffold, confocal images of both untreated and hydrolyzed, FN-coated superior and inferior surfaces were compared. After 24 h, PDL cells cultured on hydrolyzed, FN-coated surface were able to migrate into inferior surface (Fig. 6D-ii). Nevertheless, from quantitative results from resazurin assay, no significant difference was observed either in untreated or in hydrolyzed, FN-coated surfaces for 24 h (Fig. 6E).

Discussion

PDL is part of periodontium, and in certain drastic cases such as chronic periodontitis, the PDL-damaged tissue may not be repaired by classical dental therapies. TE and designed polymer biomaterials may give the mechanical support for the PDL regeneration with adapted scaffold degradability.[1,3,11] The use of designed and functionalized scaffolds may be an alternative strategy to accelerate the PDL regeneration *in situ*. In this sense, we have therefore carried out preliminary experiments to fabricate a novel scaffold based on PLGA polyester as potential biomaterial for *in situ* PDL TE. The modifications of material under humid conditions have been evaluated. Because of its hydrophobic nature, we have developed a simple method to functionalize the PLGA fibers in order to reduce their contact angle and to

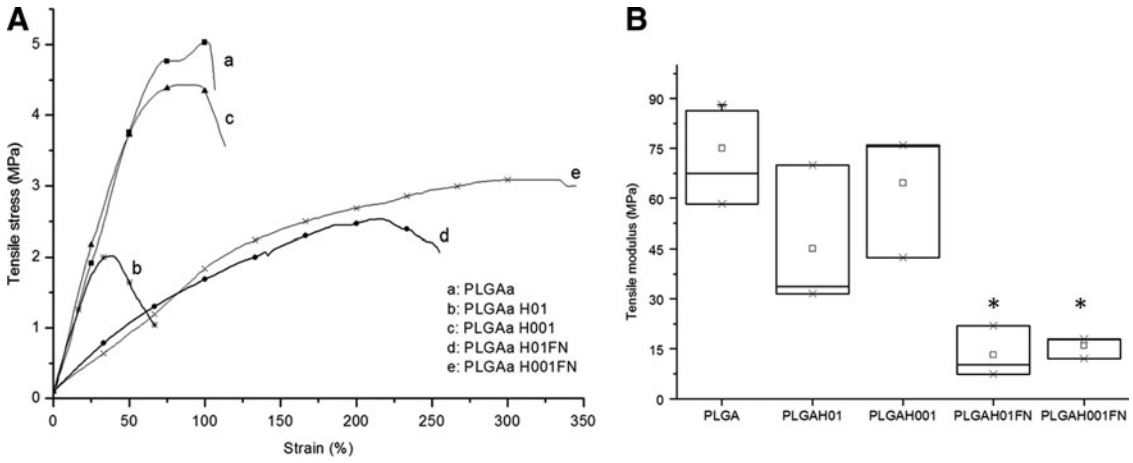

FIG. 4. Mechanical characterization of untreated, hydrolyzed, and hydrolyzed-and-coated PLGA scaffolds: **(A)** Tensile stress (MPa) versus strain (%) curves and **(B)** tensile modulus (MPa). Data are expressed as mean ± SD. *Significant difference between groups ($p < 0.05$).

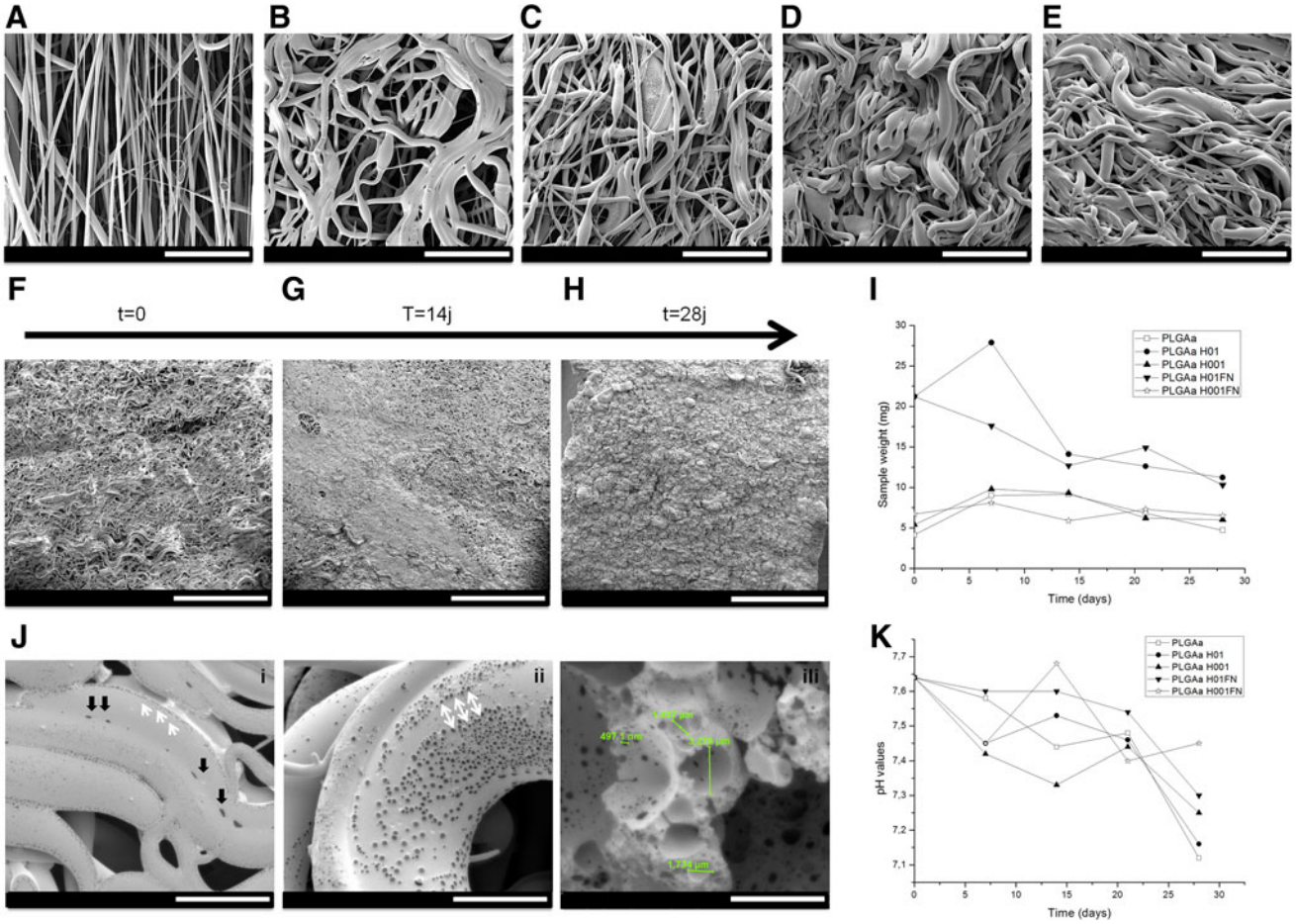

FIG. 5. Study of PLGA scaffold degradation in PBS at 37°C up to 28 days. **(A–E)** SEM micrographs of PLGA group weekly observed. Degradation behavior of PLGAH001FN samples up to **(F)** 7, **(G)** 14, and **(H)** 21 days. **(J i–iii)** Details of fiber agglutination (black arrows), appeared pores (white arrows), and pore dimensions of PLGAH001FN samples up to 21 days of PBS immersion. Scale bar: **(A–E)** 100 μm; **(F–H)** 1 mm; **(J i–iii)** 20 μm. **(I)** Changes of remaining weight and **(K)** variations of pH values during *in vitro* degradation up to 28 days.

improve their biocompatibility and colonization ability. The simplicity encountered in this proposed protocol for surface functionalization is adapted for the industry of medical devices.

PLGA scaffolds were fabricated by rotary co-electrospinning as a thin framework composed of PLGA fiber preferentially oriented that presented similar thickness of PDL *in vivo*. An activation process of the scaffold surface was tested followed by a simple FN deposition. From the XPS results, the maintained O/C rate of treated scaffolds showed the preservation of the original PLGA chemical structure confirmed by FT-IR spectra (Fig. 3A). Moreover, the presence of the protein coating by the nitrogen amount was evidenced (Fig. 3 and Table 2). Successive treatment resulted in collapsed fibers observed by SEM, suggesting that surface activation was greatly obtained with the suitable reduction of contact angles in hydrolyzed, FN-coated materials (Figs. 1 and 2). The wettability property of the material strongly depends on its chemistry and topography, having a close influence on cell adhesion and migration.[30] The decrease in the contact angle is caused not only by chemical treatment but also by the significant nanotopography and microstructural changes induced by the presence of protein.[23] Probably, the hydrolysis with the 0.1 M NaOH concentration (at the PLGAH01 surfaces) may provide a higher interaction with water molecules and significantly increase the remaining mass and water adsorption, demonstrating the creation of charged $COOH^-$ groups at the surface (Table 2). It is possible to affirm that alkaline hydrolysis was necessary to improve surface properties and to ensure the FN entrapment (Table 2).

Chemical reactions, increased temperature, and hydration phenomena resulted in a significant shrinkage of the PLGA scaffolds (Table 2). According to Zhou et al.,[14] a strong shrinkage may result in the surface energy changes when electrospun materials are placed at 37°C. We have observed shrinkage of dried scaffolds maintained for 4 h at 37°C (data not shown). Rotary electrospinning provides tension to fibers and the temperature could trigger fiber reorganization resulting in a lower stretched state.[27] Furthermore, the composition and different viscoelastic properties of both polyester molecules may induce heterogeneous behavior with deleterious effects.[31] The effect of fiber orientation loss and shrinkage could be also noted through the decrease in mechanical properties: for example, obtained tensile modulus from 75 ± 14 MPa for untreated PLGA samples to 15.9 ± 3.4 MPa for PLGAH001FN (Fig. 4B). Scaffolds based

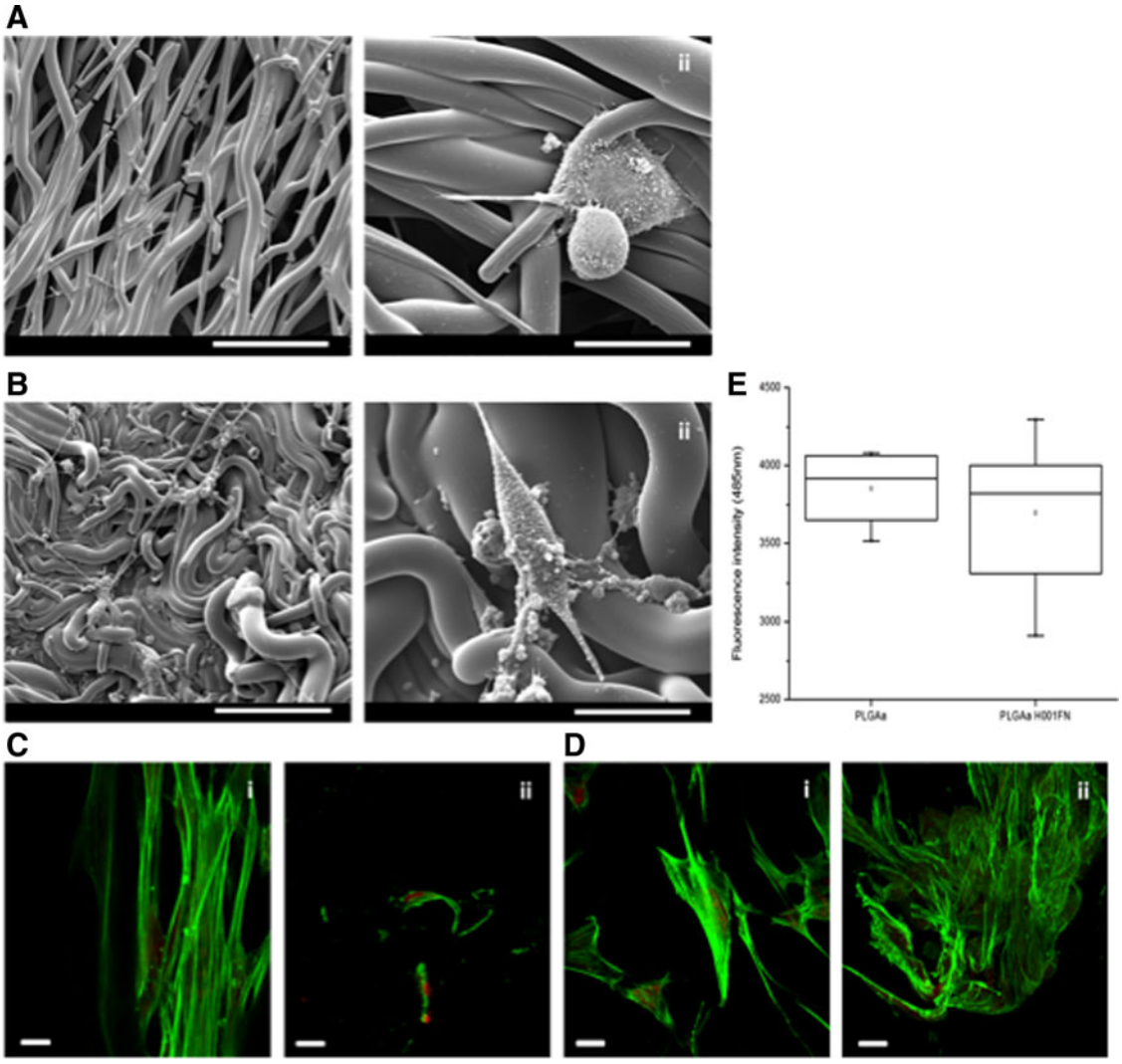

FIG. 6. Biocompatibility observations of PDL cells cultured on untreated PLGA and PLGAH001FN samples. **(A,B)** SEM micrographs of PDL-like fibroblasts cultured on **(A)** untreated PLGA [scale bar **(i)** 100 μm and **(ii)** 30 μm] and **(B)** PLGAH001FN [scale bar **(i)** 100 μm and **(ii)** 30 μm] up to 7 days. **(C,D)** Confocal images of PDL cells cultured on **(C)** untreated PLGA surface and **(D)** PLGAH001FN surfaces up to 24 h; **(i)** and **(ii)** correspond to superior and inferior surfaces of samples, respectively. Scale bar **(C,D)** 100 μm. **(E)** Quantitative resazurin results of PDL cells cultured on PLGA and PLGAH001FN samples up to 24 h. Data are expressed as mean ± SD ($n = 3$). PDL, periodontal ligament.

on PLGA have demonstrated appropriate mechanical properties for clinical uses.[11] The mechanical properties of the PDL have not been clearly described yet. Its Young's modulus has been observed to range from 10 kPa to 1750 MPa, making difficult to choose a viscoelastic biomaterial to respond to indeterminate nonlinear mechanical loading.[32]

During the periodontal cicatrization process, fibroblast-like cells and budding capillaries initiate periodontal wound healing from the first 2 days.[6] The progress of cell functions exerts different strength levels and the biomaterial should respond to the remodeling process. A synchronized ratio between material degradation and the *de novo* ECM deposition is required for maintaining the healing process and the total resorption of the biomaterial. Polyester degradation occurs with hydrolytic reactions leading to a structural deformation allowing the water ions to penetrate into the fiber chains and resulting in a higher amount of broken fibers.[31] Despite the strong shrinkage reported in the present study, the degradation properties of untreated and PLGA-treated scaffolds up to 28 days have shown that these materials are appropriate to use in PDL regeneration.[33]

The synergistic effect between the surface functionalization using bioactive molecules and the engineered scaffold structure for cell guidance has shown good results as observed for other applications. Meng et al.[20] have improved the hydrophilicity of PLGA electrospun membranes by gelatin entrapment to increase neural stem cell proliferation; Chen et al.[21] have degraded PLGA membranes by hydrolysis and created specific binding sites using dopamine to improve osteoblast viability; Qin et al.[34] have varied FN concentration to optimize tenocyte growth on PLGA substrates; and Yao et al.[35] have coated PLGA scaffolds with collagen type I or laminin to ameliorate neurite growth. From the biocompatibility results, the FN deposition has greatly improved

the cell behavior and the scaffold colonization (Fig. 6). By SEM, abnormal morphology of PDL cells was observed in contact with untreated materials (Fig. 6A). Shi et al.[25] demonstrated the effect of an FN gradient on electrospun surfaces not only on cell–scaffold interactions but also on the spreading behavior. However, cell quantitative results did not show significant differences between untreated PLGA and PLGAH001FN scaffolds (Fig. 6I). Observing confocal images, PDL cells were able to adhere and migrate to inferior surface through the PLGA scaffolds on both samples (Fig. 6C,D). Nevertheless, the most important migration was visualized at PLGAH001FN samples. Enhancing the biocompatibility of PLGA substrates could greatly promote cells' adhesion into the scaffolds. Inanç et al.[19] have also observed that PDL cells cultured in contact with PLGA electrospun scaffolds without treatment exhibit a round shape during the first 48 h.

Conclusions

We have developed a simple functionalization method to create a biocompatible electrospun PLGA scaffold for soft TE. The performed alkaline hydrolysis was able to entrap FN molecules, resulting in decreased hydrophobicity and increased biocompatibility of PLGA scaffolds, conserving their mechanical properties. Scaffold degradation behavior is suitable for periodontal TE. Under physiological environments, functionalized PLGA scaffolds may provide structural and viscoelastic resistance during tissue wound healing. Clinically, these scaffolds would be an easily handled biomaterial for routine manipulation in periodontal surgery procedures.

Acknowledgments

The authors would like to thank Lyon Science Transfert for financial support, the Biomaterials Laboratory at the University of Geneva for providing hPDL fibroblasts, the Centre Technologique des Microstructures of Lyon 1 (CTμ) for access to the SEM, Olympus Company for confocal microscopy disponibility, and Science et Surface Company for XPS analyses.

Author Disclosure Statement

No competing financial interests exist.

References

1. Vaquette C, Fan W, Xiao Y, et al. A biphasic scaffold design combined with cell sheet technology for simultaneous regeneration of alveolar bone/periodontal ligament complex. Biomaterials. 2012;33:5560–5573.
2. Chang NJ, Lin CC, Li CF, et al. The combined effects of continuous passive motion treatment and acellular PLGA implants on osteochondral regeneration in the rabbit. Biomaterials. 2012;33:3153–3163.
3. Reis ECC, Borges APB, Araujo MVF, et al. Periodontal regeneration using a bilayered PLGA/calcium phosphate construct. Biomaterials. 2011;32:9244–9253.
4. Slots J. Periodontology: past, present, perspectives. Periodontology 2000. 2013;62:7–19.
5. Susin C, Wikesjo UME. Regenerative periodontal therapy: 30 years of lessons learned and unlearned. Periodontology 2000. 2013;62:232–242.
6. Ramseier CA, Rasperini G, Batia S, et al. Advanced reconstructive technologies for periodontal tissue repair. Periodontology 2000. 2012;59:185–202.
7. Torii D, Konishi K, Watanabe N, et al. Cementogenic potential of multipotential mesenchymal stem cells purified from the human periodontal ligament. Odontology. 2014. [Epub ahead of print]; doi: 10.1007/s10266-013-0145-y.
8. Hynes K, Menicanin D, Gronthos S, et al. Clinical utility of stem cells for periodontal regeneration. Periodontology 2000. 2012;59:203–227.
9. Chen FM, Sun HH, Lu H, et al. Stem cell-delivery therapeutics for periodontal tissue regeneration. Biomaterials. 2012; 33:6320–6344.
10. Inanc B, Elcin AE, Elcin YM. Osteogenic induction of human periodontal ligament fibroblasts under two- and three-dimensional culture conditions. Tissue Eng. 2006;12:257–266.
11. Scheller EL, Krebsbach PH, Kohn DH. Tissue engineering state of art in oral rehabilitation. J Oral Rehabil. 2009;36: 368–389.
12. Sun HH, Qu TJ, Zhang XH, et al. Designing biomaterials for *in situ* periodontal tissue regeneration. Biotechnol Prog. 2011;28:3–20.
13. Armentano I, Dottori M, Fortunati E, et al. Biodegradable polymer matrix nanocomposites for tissue engineering: a review. Polymer Degradation Stability. 2010;95:2126–2146.
14. Zhou X, Cai Q, Yan N, et al. *In vitro* hydrolytic and enzymatic degradation of nestlike-patterned electrospun poly(D,L-lactide-co-glycolide) scaffolds. J Biomed Mater Res A. 2010;95:755–765.
15. Yang Y, Zhao Y, Tang G, et al. *In vitro* degradation of porous poly(L-lactide-*co*-glycolide)/β-tricalcium phosphate (PLGA/β-TCP) scaffolds under dynamic and static conditions. Polymer Degradation Stability. 2008;93:1838–1845.
16. Meng ZX, Wang YS, Ma C, et al. Electrospinning of PLGA/Gelatin randomly-oriented and aligned nanofibers as potential scaffold in tissue engineering. Mater Sci Eng C. 2010; 30:1204–1210.
17. Jose MV, Thomas V, Johnson KT, et al. Aligned PLGA/HA nanofibrous nanocomposite scaffolds for bone tissue engineering. Acta Biomater. 2009;5:305–315.
18. Kim SJ, Jang DH, Park WH, et al. Fabrication and characterization of 3-dimensional PLGA nanofiber/microfiber composite scaffolds. Polymer. 2010;51:1320–1327.
19. Inanç B, Arslan E, Seker S, et al. Periodontal ligament cellular structures engineered with electrospun poly(DL-lactide-*co*-glycolide) nanofibrous membrane scaffolds. J Biomed Mater Res A. 2009;90:186–195.
20. Meng ZX, Zeng QT, Sun ZZ, et al. Immobilizing natural macromolecule on PLGA electrospun nanofiber with surface entrapment and entrapment-graft techniques. Colloids Surf B Biointerfaces. 2012;94:44–50.
21. Chen G, Xia Y, Luoli L, et al. Effects of surface functionalization of PLGA membranes for guided bone regeneration on proliferation and behavior of osteoblasts. J Biomed Mater Res A. 2013;101:44–53.
22. Zhu AP, Fang N, Chan-Park MB, et al. Adhesion contact dynamics of 3T3 fibroblasts on poly(lactide-*co*-glycolide acid) surface modified by photochemical immobilization of biomacromolecules. Biomaterials. 2006;27:2566–2576.
23. Nagai M, Hayakawa T, Makimura M. Fibronectin immobilization using water-soluble carbodiimide on poly-L-lactic acid enhancing initial fibroblast attachment. J Biomater Appl. 2006;21:33–47.

24. Lai Y, Chen J, Zhang T, et al. Effect of 3D microgroove surface topogravy on plasma and cellular fibronectin of human gingival fibroblasts. J Dent. 2013;41:1109–1121.
25. Shi J, Wang L, Zhang F, et al. Incorporating protein gradient into electrospun nanofibers as scaffolds for tissue engineering. Appl Mater Interfaces. 2010;2:1025–1030.
26. Zhang Y, Chai C, Jiang XS, et al. Fibronectin immobilized by covalent conjugation or physical adsorption shows different bioactivity on aminated-PET. Mater Sci Eng C. 2007;27:213–219.
27. Badrossamay MR, Balachandran K, Capulli AK, et al. Engineering hybrid polymer-protein super aligned nanofibers via rotary jet spinning. Biomaterials. 2014;35:3188–3197.
28. Croll TI, O'Connor AJ, Stevens GW et al. Controllable surface modification of poly(lactic-co-glycolic acid) (PLGA) by hydrolysis or aminolysis I: physical, chemical, and theoretical aspects. Biomacromolecules. 2004;5:463–473.
29. Ayres C, Bowlin GL, Henderson SC, et al. Modulation of anisotropy in electrospun tissue-engineering scaffolds: analysis of fiber alignment by the fast Fourier transform. Biomaterials. 2006;27:5524–5534.
30. Cortese B, Riehle MO, D'Amone S, et al. Influence of variable substrate geometry on wettability and cellular responses. J Colloid Interface Sci. 2013;394:582–589.
31. Li P, Feng X, Jia X, et al. Influences of tensile load on *in vitro* degradation of an electrospun poly(L-lactide-*co*-glycolide) scaffold. Acta Biomater. 2010;6:2991–2996.
32. Saminathan A, Vinoth KJ, Low HH, et al. Engineering three-dimensional constructs of the periodontal ligament in hyaluronan-gelatin hydrogel films and a mechanically active environment. J Periodont Res. 2013;48:790–801.
33. Shue L, Yufeng Z, Mony U. Biomaterials for periodontal regeneration. Biomatter 2012;2:271–277.
34. Qin TW, Yang ZM, Wu ZZ, et al. Adhesion strength of human tenocytes to extracellular matrix component-modified poly(DL-lactide-*co*-glycolide) substrates. Biomaterials. 2005; 26:6635–6642.
35. Yao L, Wang S, Cui W, et al. Effect of functionalized micropatterned PLGA on guided neurite growth. Acta Biomater. 2009;5:580–588.

Address correspondence to:
Doris M. Campos, PhD
Laboratoire des Multimatériaux et
Interfaces CNRS UMR 5615
UFR d'Odontologie
Université Claude Bernard Lyon 1
11 rue Guillaume Paradin
Lyon 69372
France

E-mail: doris.moura-campos@univ-lyon1.fr

Abbreviations Used

ATR-FT-IR = attenuated total reflectance Fourier transform infrared
DCM = dichloromethane solvent
ECM = extracellular matrix
FN = fibronectin
hPDL = human periodontal ligament
PBS = phosphate buffered saline
PLA = poly(L-lactide)
PLGA = poly(D,L-lactide-co-glycolide)
SEM = scanning electron microscopy
TE = tissue engineering
XPS = X-ray photoelectron spectroscopy